

# Satellite Passive Attitude Stabilization using Permanent Magnets – Dynamic Model and Simulation

Darren Pais<sup>1</sup> and Sanjay Jayaram, PhD<sup>2</sup>  
Saint Louis University, Saint Louis, Missouri, 63103

The CubeSat program provides an attractive option for launch of small pico-satellites into Low Earth Orbit (LEO) for various scientific missions. The small size, computational limitations, along with mass restrictions, present significant challenges in the design of the attitude control system for such satellites. As a result, passive attitude stabilization involving gravity-gradient methods, permanent magnet alignment and/or viscous dampers, etc., are frequently considered for such missions. Passive techniques pose significantly reduced risk of failure, consume minimum on-board computational power and are very effective in LEO environments. Existing literature on studying the attitude dynamics of satellites stabilized using permanent magnets employ Euler transformation matrices and equations of motion to simulate the dynamics. While such methods provide us with a description of the attitude of the satellite as a function of time, the expressions for angular velocities obtained suffer from singularities as roll, pitch or yaw angles pass through 90°. In this paper, we investigate ways of solving such singularity issues by describing the attitude of an orbiting satellite using *Quaternions*. In addition, the techniques involved in the dynamic simulation of magnetic hysteresis damping for a satellite are also studied. To this end, a Quaternions-based mathematical model for satellite motion involving permanent magnets and hysteresis effects is presented.

## Nomenclature

${}^{\alpha}T^{\beta}$	= 3x3 transformation matrix from frame $\alpha$ to frame $\beta$
$\phi, \theta, \psi$	= roll, pitch and yaw angles respectively
$X, Y, Z$	= co-ordinate frame representation for the inertial reference frame
$x, y, z$	= co-ordinate frame representation for the moving frame
$b_1, b_2, b_3$	= co-ordinate frame representation for the body frame
$\omega_{\alpha \beta}$	= angular velocity of frame $\alpha$ with respect to frame $\beta$ , expressed in body co-ordinates
$M_{ext}$	= externally applied (magnetic) moment expressed in body coordinates
$I_B$	= moment of inertia tensor of the satellite expressed in body coordinates, centered on the satellite
$\vec{\mu}_B$	= 3x1 magnetic dipole moment vector
$\vec{B}_{\alpha}$	= external magnetic field vector expressed in frame $\alpha$
$H$	= hysteresis material magnetizing field
$B$	= hysteresis material magnetic induction
$S(t)$	= state vector for the system at a given time $t$
$q$	= 4 element (1 scalar and 3 vector) Quaternion representation of attitude

## I. Introduction

THE method of attitude control for Low Earth Orbiting (LEO) satellites must be selected between a completely passive system, or an active control system that produces the desired control torque based on signals indicating deviation from desired attitude, or a combination thereof. In satellite applications where a high degree of attitude precision is necessary (camera pointing for example), active control techniques must be employed, involving a

<sup>1</sup> Undergrad. Senior, Dept of Aerospace & Mech. Eng., 3450 Lindell Blvd, St Louis, MO. Student Member AIAA.

<sup>2</sup> Asst Professor, Dept of Aerospace & Mechanical Engineering, 3450 Lindell Blvd, St Louis, MO. Member AIAA.

collection of sensors, actuators and computer processing. However, many satellite applications exist<sup>1-4</sup> where the attitude restrictions are not as stringent, and the attitude control system plays the functional role of stabilizing the vehicle and achieving desired orientation for tasks such as antenna pointing and communication. In such applications, completely passive attitude stabilization renders itself as the most suitable option, as long as the operator is willing to sacrifice loss in robust pointing accuracy for a system with significant savings in weight, computational power, system complexity, reliability and system longevity. This trade-off becomes extremely critical in small nano- and pico-class satellites such as *CubeSats*,<sup>5</sup> where constraints of mass, volume and power are significant. Various forms of passive attitude stabilization exist,<sup>6</sup> particularly common of which are gravity-gradient methods, nutation damping and permanent magnet alignment. In this paper, we present the tools necessary to model passive satellite attitude stabilization using permanent magnets and hysteresis magnetic dampers. Magnet-based satellite stabilization presents significant savings of mass and complexity when compared to active methods, and even relative to other passive techniques such as gravity-gradient stabilization. A key drawback of the system, however, is that spacecraft attitude about the permanent magnet axis is difficult to control.

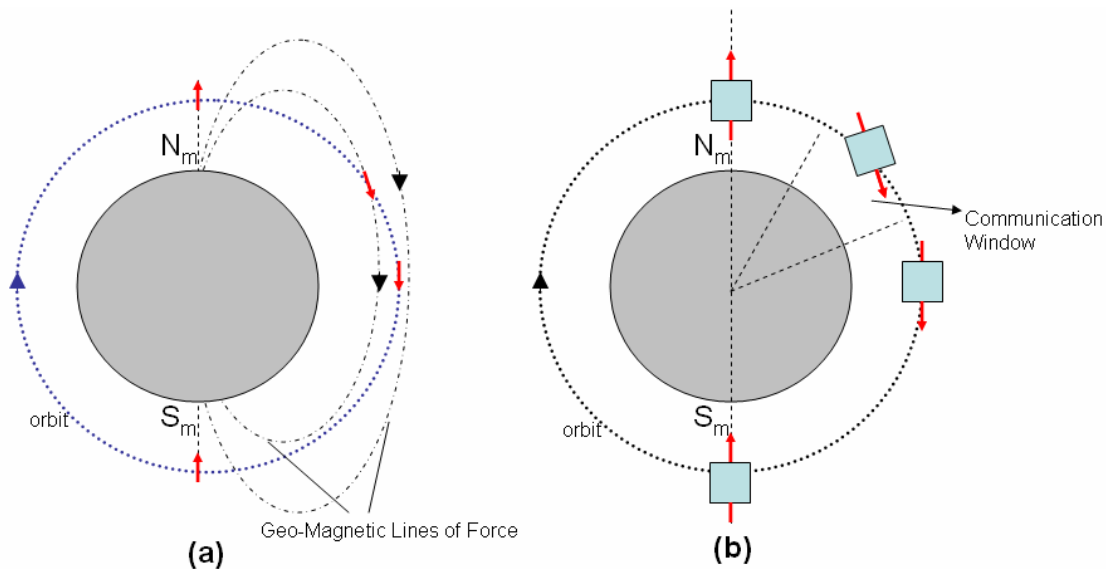


**Figure 1. a) An illustration of the Earth’s magnetic lines of force.  $N_m$  and  $S_m$  indicate the magnetic north and south poles respectively and the red arrows illustrate a permanent magnet aligning with the geo-magnetic lines of force, along a circular orbit. b) An illustration of a typical CubeSat, showing the magnet axis (red arrow) alignment for a circular orbit. The communication window indicates favorable orientation of satellite at low latitudes for communication (think of the red arrow as an antenna oriented parallel to the Earth’s surface). Figure not to scale.**

The idea behind permanent magnet based attitude stabilization is centered on the fact that a magnet will align its magnetic dipole axis with the external magnetic field direction, in the absence of other external forces, as depicted in Fig. 1. The geo-magnetic field at LEO conditions (200 - 2000 km altitude) is strong enough to interact with onboard permanent magnets and produce the necessary alignment torque. In this paper, we look at the differential equations necessary to model this magnetic alignment and ultimately present the Quaternion form of attitude representation. Further, in order to ensure that large amplitude oscillations and high angular velocities are mitigated in orbit, an energy damping mechanism is necessary. We use soft magnet hysteresis dampers, oriented on axes perpendicular to the permanent magnets, in order to achieve this dissipation. The equations to dynamically model magnetic hysteresis are presented, thereby providing us with a complete dynamic description of passive magnetic attitude stabilization.

## II. Reference Frames

A first step in simulating satellite dynamics is to define the co-ordinate reference frames relative to which we will model the attitude of the satellite. We consider three key reference frames here- 1) The Inertial Reference Frame (*IRF*), 2) The Moving Reference Frame (*MRF*), and 3) The Body Reference Frame (*BRF*).

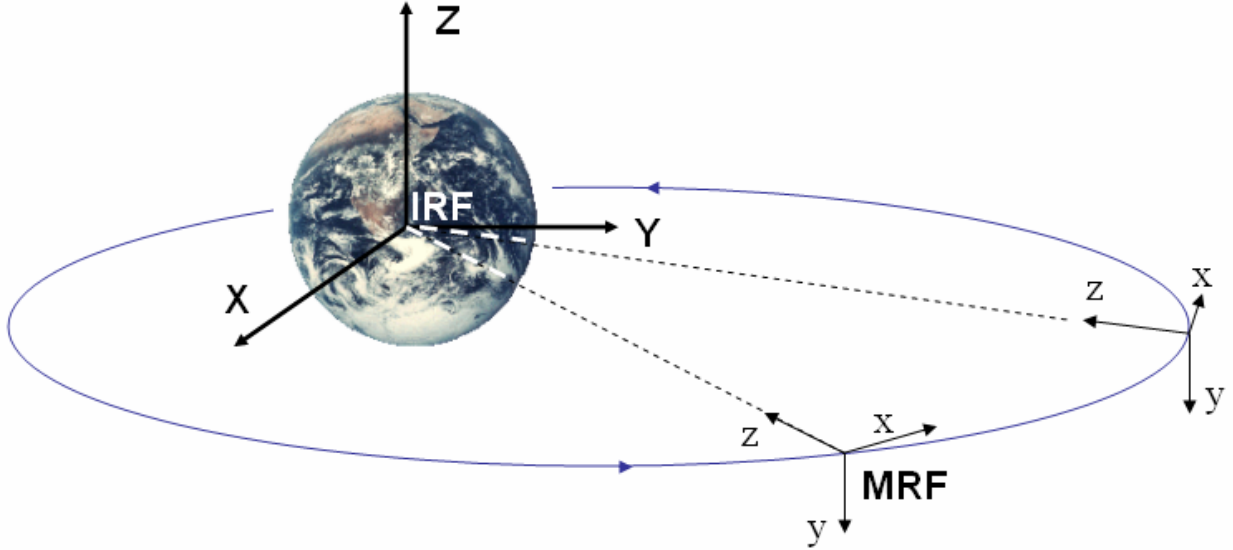


**Figure 2. Reference Frames.** IRF is the Earth centered Inertial Reference Frame denoted by XYZ and MRF is the orbit referenced Moving Reference Frame denoted by xyz. The figure depicts the MRF frame relative to the IRF frame at two different points in a given orbit.

The IRF is centered at the geometric center of the Earth and is stationary relative to the stars. An IRF referenced co-ordinate denoted by (X, Y, Z) corresponds to a given latitude, longitude and height, relative to the Earth's surface. The X-axis points in the direction of the vernal equinox, the Z-axis in the Zenith direction, and the Y-axis completes the right-handed frame. The MRF is centered at a point on the orbit, with the z-axis pointing towards the Earth's center (Nadir pointing), the x-axis pointing perpendicular to the z-axis, in the direction of orbital motion, and the y-axis completing the frame (Fig. 2). The relationship between the IRF and MRF depends on the parameters of the chosen orbit, but for simplicity, we choose a circular polar orbit as the desired reference orbit for simulations. Since the Earth's magnetic field is symmetric about the Z-axis, we restrict our orbit to the XZ plane, originating at the North Pole. Under these restrictions, the orbit can be depicted as shown in Fig. 3, with the complement of the planar inclination angle denoted by ' $\delta$ ' as the key reference parameter. From observations in Fig. 3, we can relate the IRF to the MRF via the parameter  $\delta$  and a suitable 3x3 transformation matrix  ${}^I T^M$ , as presented in Eq. (1).

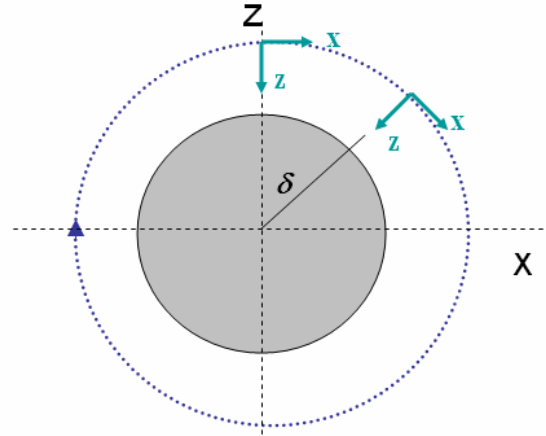


**Figure 3. Relationship between IRF and MRF for a circular polar orbit in the XZ plane, where the complement of the planar inclination angle represented by  $\delta$  is the key reference parameter.**

$$\begin{pmatrix} x \\ y \\ z \end{pmatrix} = \begin{bmatrix} \cos \delta & 0 & -\sin \delta \\ 0 & -1 & 0 \\ -\sin \delta & 0 & -\cos \delta \end{bmatrix} \begin{pmatrix} X \\ Y \\ Z \end{pmatrix} \quad (1)$$

It is important to note here that Eq. (1) presents an IRF to MRF transformation for the *particular* orbit type chosen, however, similar transformations can be constructed for other chose orbits.<sup>14</sup> Further, our choice of a circular polar orbit is of particular interest because it represents the most common orbit type for CubeSat deployments, and helps us study the response of passive magnetic attitude control for an orbit with drastic magnetic field direction changes, particularly near the poles.

The BRF is centered at the center of mass of the satellite and comprises three orthogonal axes denoted as  $b_1$ ,  $b_2$  and  $b_3$ . In our analysis, the permanent magnets have their dipoles oriented in the positive  $b_3$  direction on the satellite. The choice of BRF axes relative to the satellite may seem arbitrary, however these axes are often picked to correspond closely to the axes of principal moments of inertia of the satellite in order to render the products of inertia terms in the inertia tensor (expressed in the BRF) as zero. The relationship between the orbit-referenced MRF and body-referenced BRF is critical in studying the attitude of the satellite in orbit and is depicted in Fig. 4.

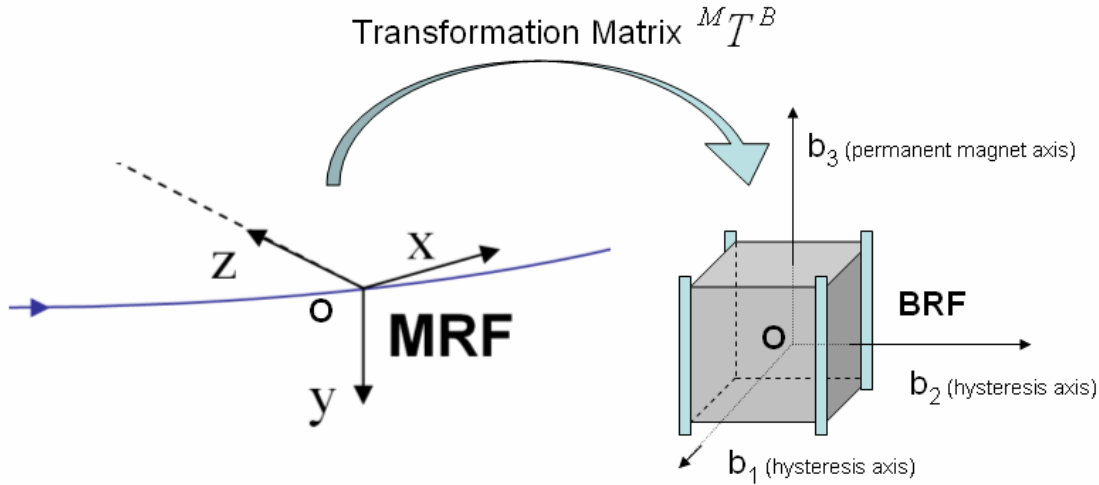


**Figure 4. Relationship between MRF and BRF for a satellite via the  $M T^B$  transformation, showing body axes that correspond to permanent magnet and hysteresis material dipole alignment.**

The matrices that relate the BRF and MRF frames are commonly called Euler Angle transformation matrices, and comprise 12 different rotational sequences producing equivalent transformations. For our purposes, we adopt the  $\theta \rightarrow \phi \rightarrow \psi$  transformation, which represents a pitch angle transformation of  $\theta$  about the y-axis, followed by a roll angle transformation  $\phi$  about the x-axis and a yaw angle transformation  $\psi$  about the z-axis. The composite 3x3-transformation matrix  $M T^B$  is presented in Eq. (2).

$$\begin{pmatrix} b_1 \\ b_2 \\ b_3 \end{pmatrix} = \begin{bmatrix} \cos \theta \cos \psi + \sin \phi \sin \theta \sin \psi & \cos \phi \sin \psi & -\sin \theta \cos \psi + \sin \phi \cos \theta \sin \psi \\ -\cos \theta \sin \psi + \sin \phi \sin \theta \cos \psi & \cos \phi \cos \psi & \sin \theta \sin \psi + \sin \phi \cos \theta \cos \psi \\ \cos \phi \sin \theta & -\sin \phi & \cos \phi \cos \theta \end{bmatrix} \begin{pmatrix} x \\ y \\ z \end{pmatrix} \quad (2)$$

As noted, the particular Euler angle transformation presented in Eq. (2) is one 12 possible choices.<sup>7</sup> The reasons behind this specific selection will become evident in Section III of this paper.

### III. Attitude Dynamics

In this section, we develop the differential equations necessary to model the orbital motion and attitude of a satellite dynamically. Numerical solutions to the differential equations presented provide us with time dependent angular velocities and attitude parameters (such as roll, pitch and yaw) with respect to the IRF or the MRF. We begin with a derivation of Euler's equation, followed by angular velocity conversions and attitude dynamics equations.

### A. Euler's Moment Equation

For an arbitrary time dependent vector  $\vec{r}$  represented in two frames as  $\vec{r}_I$  (inertial frame) and  $\vec{r}_B$  (body frame), where  $\omega_{B/I}$  represents the angular velocity of the body frame with respect to the inertial frame, the time derivative of the body frame vector is obtained using the transformation matrix  ${}^I T^B = {}^M T^B \cdot {}^I T^M$  as shown in Eq. (3).<sup>8</sup>

$$\frac{d\vec{r}_B}{dt} = -\omega_{B/I} \times \vec{r}_B + {}^I T^B \frac{d\vec{r}_I}{dt} \quad (3)$$

From Newton's second law we have that the rate of change of angular momentum of a body is equivalent to the external force acting on it, which is represented in Eq. (4), where  $\vec{L}_I$  is the angular momentum projected in the inertial frame, and  $M_{ext,I}$  is the net external moments, also projected in the inertial frame.

$$\frac{d\vec{L}_I}{dt} = M_{ext,I} \quad (4)$$

In the body reference frame, by definition the angular momentum is given by Eq. (5), where the 3x3 body mass moment of inertial tensor is represented as  $I_B$ ,

$$\vec{L}_B = I_B \omega_{B/I}. \quad (5)$$

Making substitutions using Eq. (4) and Eq. (5) in Eq. (3), we obtain Euler's moment equation expressed in the satellite BRF, as presented in Eq. (6)<sup>8</sup> (note that  $M_{ext,B} = {}^I T^B M_{ext,I}$ ).

$$\frac{d\omega_{B/I}}{dt} = I_B^{-1} \{M_{ext,B} - \omega_{B/I} \times (I_B \cdot \omega_{B/I})\} \quad (6)$$

### B. Angular Velocity Conversions, Rotating Frame Angular Velocity

For the orbital motion of the satellite as depicted in Fig. 3 (circular, polar orbit of constant orbital speed), the angular velocity of the MRF with respect to the IRF, as expressed in BRF coordinates using the  ${}^M T^B$  transformation matrix is given by Eq. (7) where  $n$  is the mean orbital motion of the satellite given by Eq. (8).

$$\omega_{M/I} = -n \begin{pmatrix} 0 \\ 1 \\ 0 \end{pmatrix} \quad (7)$$

$$n = \sqrt{\frac{\mu}{a^3}}, \text{ where Earth Gravitation Parameter } \mu = 3.986 \times 10^5 \frac{km^3}{s^2} \quad (8)$$

and  $a$ : orbit semi-major axis in kilometers.

The negative sign in Eq. (7) exists because the orbital angular velocity vector is anti-parallel to the MRF y-axis for the orbit shown in Fig. 3. The angular velocity of the BRF with respect to the MRF,  $\omega_{B/M} = \omega_1 \hat{b}_1 + \omega_2 \hat{b}_2 + \omega_3 \hat{b}_3$  can be expressed as,

$$\omega_{B/M} = \omega_{B/I} - \omega_{M/I}. \quad (9)$$

Making a substitution for Eq. (7) into Eq. (9), we obtain an expression for the angular velocity of the BRF with respect to the MRF as a function of  $\omega_{B/I}$  and the attitude transformation matrix as,

$$\begin{pmatrix} \omega_1 \\ \omega_2 \\ \omega_3 \end{pmatrix} = \omega_{B/I} + n \begin{pmatrix} 0 \\ 1 \\ 0 \end{pmatrix} \quad (10)$$

For the  $\theta \rightarrow \phi \rightarrow \psi$  transformation as defined in Eq. (2) we can obtain the BRF Euler angles rates using the system of equations,<sup>6</sup>

$$\begin{aligned}
\frac{d\theta}{dt} &= \frac{1}{\cos\phi} [\omega_1 \sin\psi + \omega_2 \cos\psi] \\
\frac{d\phi}{dt} &= [\omega_1 \cos\psi - \omega_2 \sin\psi] \\
\frac{d\psi}{dt} &= \tan\phi [\omega_1 \sin\psi + \omega_2 \cos\psi] + \omega_3
\end{aligned} \tag{11}$$

Eq. (6) can be solved numerically to obtain  $\omega_{B/I}$  at discrete time-steps. Further, using Eq. (10), we can obtain values of  $\omega_1, \omega_2$  and  $\omega_3$  at each time step. Hence, the systems of differential equations in Eq. (6) and Eq. (11) are coupled and can be solved simultaneously at discrete time-steps in order to obtain the roll, pitch and yaw angles of the satellite and thereby a description of its attitude. It is also important to note that the systems of equations are non-linear, thereby making it difficult to obtain an analytical solution without very specific constraints.<sup>6</sup> Further, for the system in Eq. (11), it is important to notice the singularities for roll angle  $\phi = 90^\circ$ . In Section V (*attitude simulation*) of this paper, we will see that the roll angle is not critical to the simulation and seldom approaches  $90^\circ$ , thereby validating our choice for the  $\theta \rightarrow \phi \rightarrow \psi$  transformation in Eq. (2). Further, in Section VI we present the *Quaternion* representation of satellite attitude that will comprise a linearized representation of Eq. (11) that does not have any singularities.

#### IV. Magnetic and Hysteresis Torques Modeling

The International Geomagnetic Reference Field (IGRF-10) provides a mathematical description of the magnetic field of the Earth as outlined in Ref. 9. The IGRF expresses the scalar magnetic potential as a series expansion function of distance from the Earth's center, latitude and longitude. The coefficients of the series expansion are obtained from fitting to satellite measurement data and normalized coefficients associated with Legendre functions. The gradient of the potential function provides the magnetic field lines of force. The DGRF/IGRF website\* provides a convenient means of obtaining the magnetic field vector in IRF coordinates ( $\vec{B}_I$ ) with suitable input of latitude, longitude and altitude. While the expressions in Ref. 9 provide an accurate and widely used technique to compute the geo-magnetic field, the approximate L-Shell model of the magnetic field helps provide a good qualitative description of the field lines.<sup>10</sup> At a given magnetic latitude  $\lambda$ , for a given  $L$ -value (measured in Earth Radii, corresponding to a given field line), the field radius  $R$ , which is the distance in Earth Radii from an idealized magnetic dipole at the Earth's center is given by,<sup>10</sup>

$$R = L \cos^2 \lambda \tag{12}$$

The Cartesian components of  $R$  along the X-axis and Z-axis are  $R \cos \lambda$  and  $R \sin \lambda$  respectively. Using Eq. 12 and plotting the magnetic field in the IRF XZ-plane, we obtain a pictorial representation of the geo-magnetic field, as shown in Fig. 5. The two sub-sections to follow illustrate the equations used to compute permanent and hysteresis magnetic torques at a point in orbit, given to local magnetic field vector at the point,  $\vec{B}_I$ .

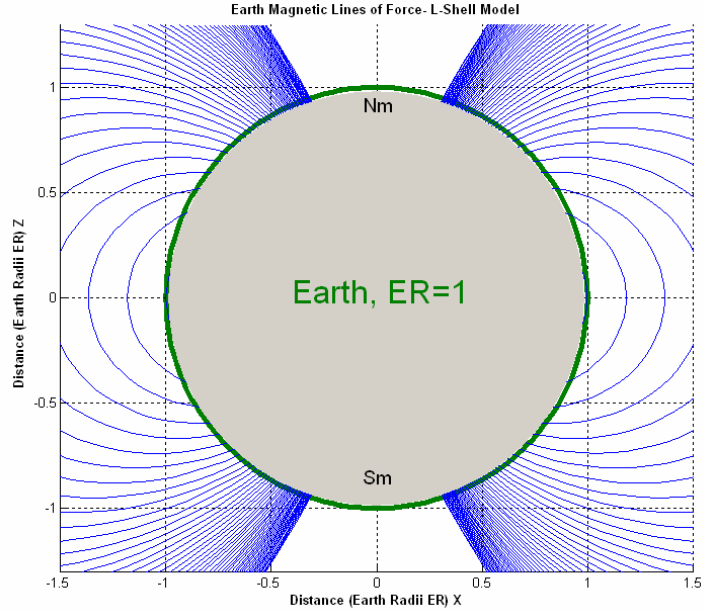


**Figure 5. Earth magnetic field lines using the L-Shell model.**

\* King, J.H., NASA GSFC, URL: <http://nssdc.gsfc.nasa.gov/space/model/models/igrf.html> [cited 10 March 2007].

### A. Permanent Magnet Torque

Assuming perfect dipole distributions of the field around a permanent magnet, the magnetic dipole moment vector  $\vec{\mu}_B$  (expressed in the BRF) can be computed knowing the magnet's rated magnetic induction  $B$  (Tesla), its volume  $V$  (cubic meters), the axis of dipole orientation (positive body  $b_3$  axis in our case), and the permeability of free space  $\mu_0 (= 4\pi \times 10^{-7} \text{ N/A}^2)$  using the expression,<sup>11</sup>

$$\vec{\mu}_B = \frac{B \cdot V}{\mu_0} \begin{pmatrix} 0 \\ 0 \\ 1 \end{pmatrix}. \quad (13)$$

The geo-magnetic field model described in Eq. (12) and Ref. 9 provides us with magnetic field vector expressed in the IRF,  $\vec{B}_I$  (Tesla). This field vector can be expressed in the BRF using the transformation matrices from Eq. (1) and Eq. (2) as,

$$\vec{B}_B = \left( {}^M T^B \cdot {}^I T^M \right) \vec{B}_I. \quad (14)$$

The external torque exerted by the permanent magnets at a given point in the orbit can now be conveniently computed using a simple cross product as,<sup>12</sup>

$$M_{perm,B} = \vec{\mu}_B \times \vec{B}_B. \quad (15)$$

### B. Hysteresis Damping Torque

Hysteresis magnetic materials are much like permanent magnets in their function, except that they are of significantly higher permeability. This means that under the influence of a changing weak external magnetic field (like the Earth's field), the hysteresis materials tend to exhibit realignment of dipoles and change in magnetic domain boundaries.<sup>11</sup> These changes result in frictional dissipation of energy at the molecular level, a phenomenon known as hysteresis dissipation. Hysteresis materials have been successfully used for damping satellite oscillations on prior missions.<sup>1-3</sup> In order to maintain system equilibrium on permanent magnet and field alignment, the hysteresis materials must have their dipole axes orthogonal to the permanent magnets (on the  $b_1$  or  $b_2$  BRF axes in our case).<sup>11</sup> Hysteresis materials are defined by three key parameters- the saturation induction  $B_m$  (Tesla), the remanent induction  $B_0$  (Tesla) and the coercivity  $H_0$  (Ampere/meter). Using these parameters, the hysteresis loop outer boundaries can be approximated as tangent functions (Eq. (16)) as illustrated in Refs. 1 and 2, and depicted in Fig. 6.

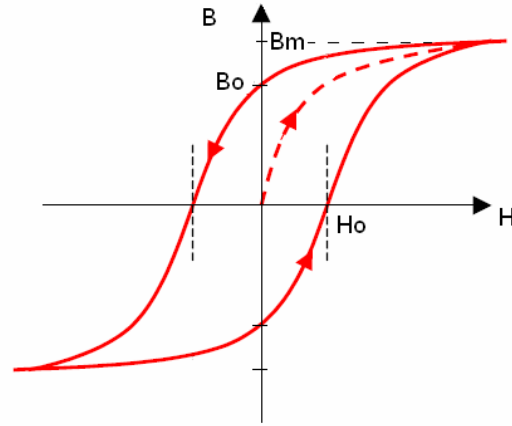


**Figure 6. Variation of magnetic induction (B) with external magnetizing field (H) for a hysteresis material.**

$$B = \frac{2B_m}{\pi} \tan^{-1} \left[ \frac{1}{H_0} \tan \left( \frac{\pi B_0}{2B_m} \right) (H \pm H_0) \right] \quad (16)$$

The expressions in Ref. 1 allow us to predict the changing magnetic induction of the hysteresis material ( $B$ ) dynamically, knowing the component of the external magnetic field ( $B_1, B_2$  (tesla)  $\rightarrow H$  (Oe, Amperes/m)) along the axis of the hysteresis material, at a point and time in orbit. Particularly, changes in the external magnetic field can be related to the magnetic induction of the hysteresis material (and thus the magnetic dipole moment) by the equation,<sup>1</sup>

$$\frac{dB}{dt} = \frac{dB}{dH} \cdot \frac{dH}{dt}. \quad (17)$$

This dynamic induction can in turn be converted to the corresponding hysteresis damping moments,  $M_{hys,B}$  using Eqs. (13) (with an x- or y-axis unit vector), (14) and (15), knowing the volume of hysteresis material used.

## V. Attitude Simulation

In this section, we present the steps involved in dynamically modeling the attitude of a passive magnetically stabilized satellite. We calculate the state of the system at discrete time steps by numerically solving the systems of differential Eqs. (6) and (11). The state of the system at a given time step can be represented by a single, time-dependent vector comprising the variables in the differential equations as,  $S(t) = [\omega_{B/I}(t) \ \phi(t) \ \theta(t) \ \psi(t)]$ . For simulations here, we restrict to the circular, polar orbit as represented in Fig. 3. The steps involved for attitude simulation are as follows:

1. Set up initial conditions for angular velocity and roll, pitch and yaw angles for the state vector at  $t = 0$ .
2. Calculate external moments at given time and orbit position using Eqs. (1), (2), (15) and (17).
3. Numerically solve differential Eq. (6) for angular velocity vector  $\omega_{B/I}(t)$  at given time.
4. Calculate the angular velocity of the BRF with respect to the MRF using Eq. (10).
5. Numerically solve the system in Eq. (11) for  $\phi, \theta$  and  $\psi$  using coefficients obtained in step 4.
6. Iterate on steps 1-5 by incrementing the time by the time step  $\Delta t$ .

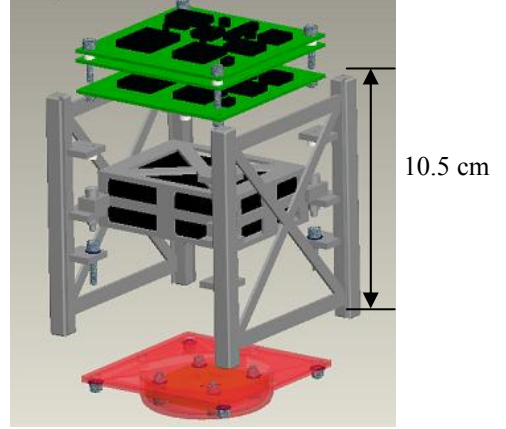


**Figure 7. BillikenSat-II showing components. The red container encloses the payload, a Bio-Fuel cell.**

We simulate the satellite attitude at a typical LEO altitude of 800km, with parameters similar to those used in Ref. 13. The hysteresis material parameters used are the same as those for the TRANSIT-1B satellite,<sup>1,3</sup>  $B_0 = 0.012$  Tesla,  $B_m = 0.25$  Tesla and  $H_0 = 0.035$  Oe. The inertia tensor used is that of BillikenSat-II configuration<sup>†</sup> (pictured in Fig. 7) after neglecting the cross terms due to axial symmetry and is given by,

$$I_B = \begin{bmatrix} 0.00182 & 0 & 0 \\ 0 & 0.00185 & 0 \\ 0 & 0 & 0.00220 \end{bmatrix} \text{kg.m}^2. \quad (18)$$

Scenario 1 of our set of simulations is for all initial conditions in the state vector  $S(t)$  (angular velocities and Euler angles) set to zero, for a satellite having only permanent magnets for stabilization and no hysteresis dampers. The results of this simulation are presented in Fig. 8 for one full orbit at different permanent magnet strengths. Notice that the higher permanent magnet strength implies a higher frequency of oscillation and higher oscillation amplitude as expected. Also, notice that the satellite does pitch through the necessary  $360^\circ$  in one orbit, illustrating that it oscillates about the geo-magnetic field with maximum amplitude of about  $20^\circ$  (Fig. 8(c) and 8(d)). In Scenario 2 (Fig. 9) we simulate the effects of adding hysteresis damping to mitigate the high-amplitude oscillations observed for the higher permanent magnetic dipole stabilization in Scenario 1 (Fig. 8). Notice the smoothing of the pitch and yaw curves, as well as the reduction in field offset, because of the mitigation of oscillations by the hysteresis materials. The hysteresis materials have a lesser long-term effect on mitigating roll oscillations as they do not exert moments along the roll axis following field alignment (because they are perpendicular to the alignment axis of the permanent magnets). However, roll oscillation amplitudes are significantly mitigated as seen in Fig. 9(a).

## VI. Quaternion Representation

Observations of the Euler angle equations presented in Section III, as well as the attitude simulations presented in Section V, raise important concerns. Firstly, the use of the dynamic simulations in an iterative satellite design process would require us to be able to impose a variety of initial conditions. This would require that the roll angle singularity in Eq. (11) be taken care of. Second, the non-linear nature of the differential equations renders them cumbersome and inefficient for computing attitude for a larger number of orbits. In order to overcome these limitations, we have chosen to adopt the Quaternion approach to modeling the attitude of the satellite.

<sup>†</sup> Project at the Space Systems Research Lab. of Saint Louis U. URL: <http://cubesat.slu.edu> [cited 12 March 2007].

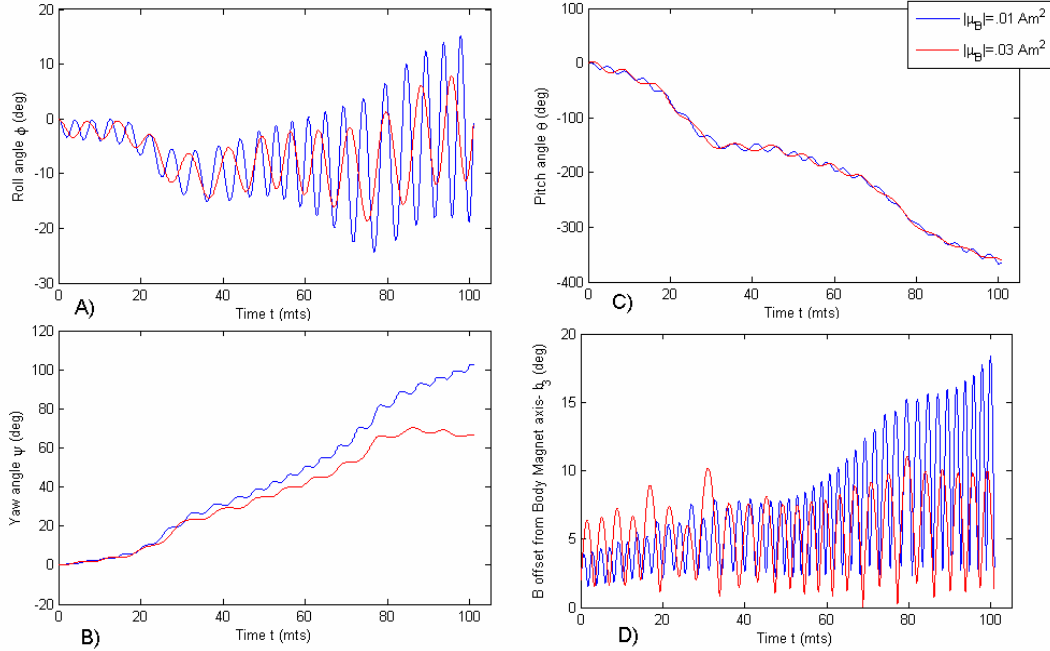


**Figure 8. Scenario 1-Permanent magnet response a) Roll angle response b) Yaw angle response c) Pitch angle response d) B-offset: magnet deviation from field lines, notice higher amplitudes and oscillation frequencies for higher magnetic dipole moment (curves in red). Dipoles: Blue  $0.03 \text{ Am}^2$ , Red:  $0.01 \text{ Am}^2$ .**

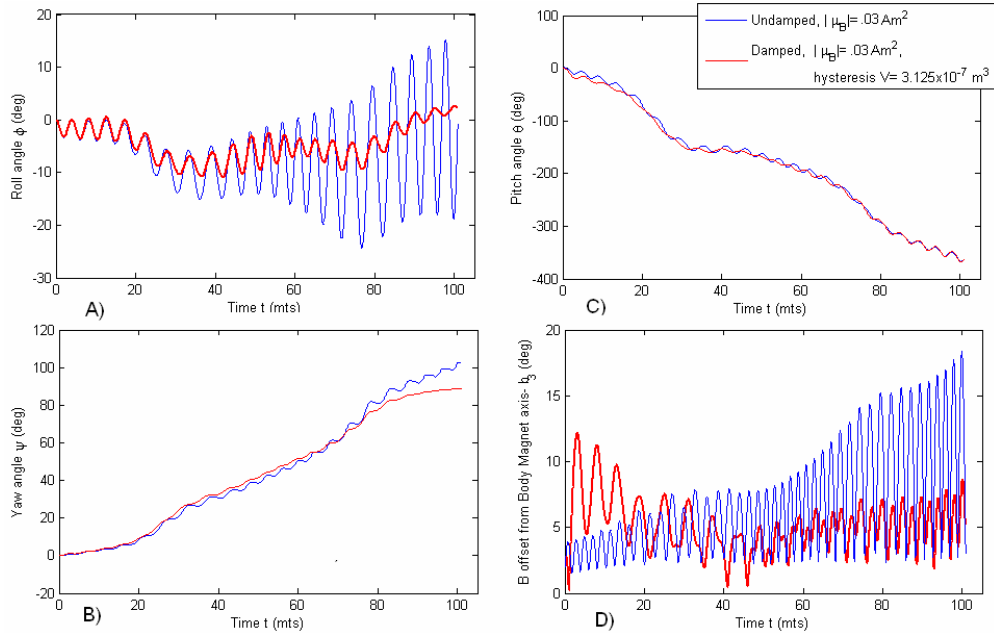


**Figure 9. Scenario 2-Permanent magnet with hysteresis response a) Roll angle response b) Yaw angle response c) Pitch angle response d) B-offset, notice yaw and pitch damping, roll amplitude mitigation (red)**

Quaternions may be regarded as a 4-tuple of real numbers (i.e. an element of  $\mathbb{R}^4$ ) and are typically represented by the letter  $\mathbf{q}$ , as a combination of a vector in  $\mathbb{R}^3$  and a scalar ( $\mathbf{q} = q_0 + q_1\hat{i} + q_2\hat{j} + q_3\hat{k}$ ). Geometrically, Quaternions can be related to rotations about a unit vector axis  $\vec{u} \in \mathbb{R}^3$  by an angle  $\theta$  using the relationship,

$$\mathbf{q} = \cos \theta + \vec{u} \sin \theta \quad (19)$$

Details of Quaternion conjugation, multiplication and rotation are presented in Ref. 7. Here, we present the key relationships necessary for modeling the system at hand. For the  $\theta \rightarrow \phi \rightarrow \psi$  transformation, Quaternions are related to Euler angles by the relationships,

$$\begin{aligned} q_0 &= \cos \phi \cos \theta \cos \psi + \sin \phi \sin \theta \sin \psi \\ q_1 &= \sin \phi \cos \theta \cos \psi + \cos \phi \sin \theta \sin \psi \\ q_2 &= \cos \phi \cos \theta \sin \psi - \sin \phi \sin \theta \cos \psi \\ q_3 &= \cos \phi \sin \theta \cos \psi - \sin \phi \cos \theta \sin \psi \end{aligned} \quad (20)$$

Further, the rotation matrix can be derived from Quaternions using the expression in Eq. (21).<sup>7</sup> Here we see that a given Quaternion is analogous to a set of Euler angles in providing the necessary rotation matrix for transformations.

$${}^M T^B = \begin{bmatrix} q_1^2 - q_2^2 - q_3^2 + q_0^2 & 2(q_1 q_2 + q_0 q_3) & 2(q_1 q_3 - q_0 q_2) \\ 2(q_1 q_2 - q_0 q_3) & -q_1^2 + q_2^2 - q_3^2 + q_0^2 & 2(q_2 q_3 + q_0 q_1) \\ 2(q_1 q_3 + q_0 q_2) & 2(q_2 q_3 - q_0 q_1) & -q_1^2 - q_2^2 + q_3^2 + q_0^2 \end{bmatrix} \quad (21)$$

In order to use Quaternions to simulate satellite attitude dynamically we need a system of differential equations to replace the Euler angle system in Eq. (11). This is given by,<sup>6</sup>

$$\frac{d}{dt} \begin{pmatrix} q_1 \\ q_2 \\ q_3 \\ q_0 \end{pmatrix} = \frac{1}{2} \begin{bmatrix} 0 & \omega_3 & -\omega_2 & \omega_1 \\ -\omega_3 & 0 & \omega_1 & \omega_2 \\ \omega_2 & -\omega_1 & 0 & \omega_3 \\ -\omega_1 & -\omega_2 & -\omega_3 & 0 \end{bmatrix} \begin{pmatrix} q_1 \\ q_2 \\ q_3 \\ q_0 \end{pmatrix}. \quad (22)$$

Hence, using Eqs. (6) and (22), and expressing the attitude of the satellite in the Quaternion form (Eq. (21)), we can model the satellite attitude in the absence of any singularities. Further, the system in Eq. (22) is linear and is hence computationally more efficient. In Fig. 10, we present the results of a specific modeling scenario using the Quaternion equations. We simulate similar initial conditions as that of Scenario 1 (Fig. 8, all initial conditions zero) with the exception that we induce an initial deployment angular velocity of 0.2 rpm along the body  $b_3$  (z-axis) and observe the response for undamped oscillation, and further illustrate the mitigation of induced high-amplitude oscillations using hysteresis damping.

## VII. Conclusion

The combination of hysteresis and permanent magnetic material is an effective method of controlling the attitude of satellite in LEO conditions, particularly for satellites that do not demand rigorous pointing accuracy. The differential equations presented provide the necessary tools to model the attitude of the satellite dynamically. Further, the equations presented by Kumar et al.<sup>1</sup> enable us to dynamically model the non-linear hysteresis effect. Combining these expressions, we are able to model the attitude of a damped satellite in orbit, illustrating the effects of adding hysteresis damping to a permanent magnet stabilized system. It is important to note that though the simulations presented here are restricted to a simple polar, circular orbit for simplicity, they can be generalized to simulate any given Earth orbit via appropriate transformations. Further, the Quaternion form of the dynamical equations is presented in order to overcome the singularity and complexity disadvantages associated with the Euler angle equations. The linear, non-singular Quaternion differential equations present a convenient and efficient representation of the satellite attitude and can be used to model a variety of initial conditions for an extended number of orbits. In this paper, we present the tools necessary for modeling passive magnetically stabilized satellite dynamics; the implementation of these techniques for a specific satellite mission would require a parametric study of the various variables involved including different initial conditions, moments of inertial, orbit altitudes and orbit parameters. The final system configuration must be a balance between hysteresis material strength and permanent magnet strength to ensure that the satellite is capable of locking onto the geo-magnetic field, while at the same time stable in oscillations. This trade-off can be performed by observing the B-offset curves and setting thresholds on offset magnitude and oscillation frequency for simulations. Finally, we conclude that passive magnetic attitude control is an efficient, reliable and inexpensive technique, particularly suited to the stringent mass, volume, computation and cost restrictions of CubeSat and other nano- and pico-satellite missions.

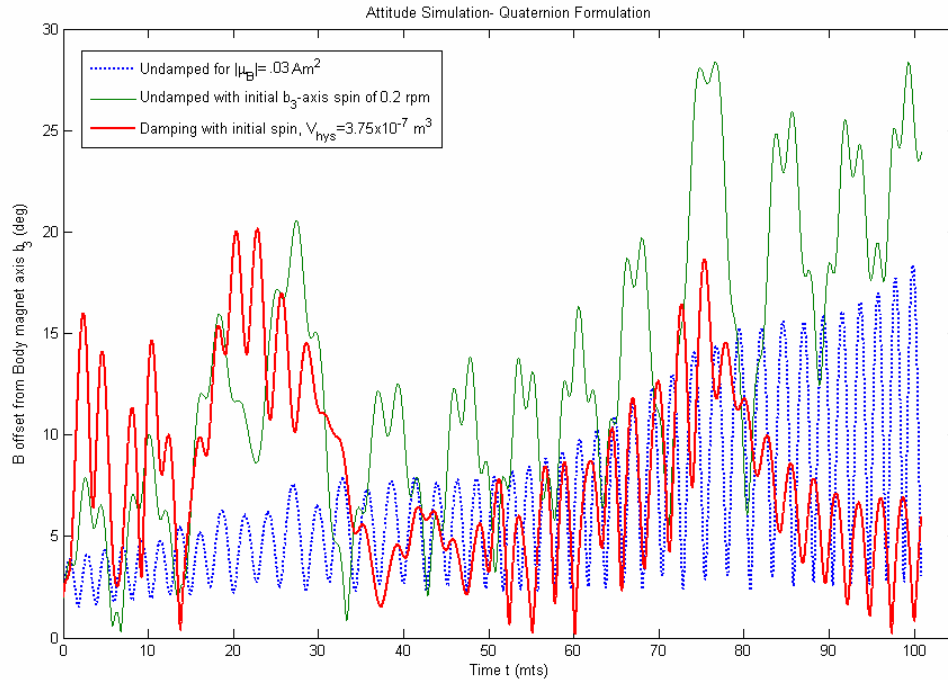


**Figure 10. Quaternion Formulation.** The dotted blue curve illustrates the magnetic field offset for a zeros initial condition vector, undamped scenario and permanent magnetic dipole strength of  $0.03 \text{ Am}^2$  (similar to blue curve in Fig. 8(d)). The green curve represents the addition of a moderate initial deployment spin of 0.2 rpm for the same dipole moment in undamped conditions. The red curve illustrates the mitigation of the initial permanent magnet axis spin using hysteresis materials of volume  $3.75 \times 10^{-7} \text{ m}^3$ .

### Acknowledgments

The authors would like to acknowledge support from the Saint Louis University (SLU) Beaumont research grant for this work. In addition, we are grateful to Prof. Krishnaswamy Ravindra and Prof. John George (Parks College, SLU) for their invaluable advice and continued support of BillikenSat-II. We are also grateful to our colleagues at the Space Systems Research Lab. (Paul Lemon, Sonia Hernandez and Nathaniel Clark) for their encouragement.

### References

- <sup>1</sup>Kumar, R. R., Mazanek, D. D., and Heck, M. L., "Simulation and Shuttle Hitchhiker Validation of Passive Satellite Aerostabilization," *AIAA Journal of Spacecraft and Rockets*, Vol. 32, No. 5, 1995 pp. 806-811.
- <sup>2</sup>Whisnant, J. M., Anand, D. K., Psiacane, V. L., and Sturmanis, M., "Dynamic Modeling of Magnetic Hysteresis," *AIAA Journal of Spacecraft and Rockets*, Vol. 7, No. 6, 1970 pp. 697-701.
- <sup>3</sup>Fischell R. E., "Magnetic Damping of the Angular Motions of Earth Satellites," *ARS Journal*, Vol. 31, No. 9, 1961 pp. 1210.
- <sup>4</sup>Waydo, S., Henry, D., and Campbell, M., "CubeSat Design for LEO-Based Earth Science Missions," *IEEE Journal*, IEEEAC paper #248, 0-7803-7231-X/01, 2002.
- <sup>5</sup>Nason, I., Puig-Surai, J., Twiggs, R., "Development of a Family of Pico-Satellite Deployers based on the CubeSat Standard," *IEEE Journal*, 0-7803-7231-X, 2002.
- <sup>6</sup>Sidi, M. J., *Spacecraft Dynamics and Control*, Cambridge, New York, 2005, Chap. 4, 6 and 7.
- <sup>7</sup>Kuipers J. B., *Quaternions and Rotation Sequences*, Princeton University Press, Princeton NJ, 1999, Chaps. 4, 6, 7 and 11.
- <sup>8</sup>Pisacane, V. L., *Fundamentals of Space Systems*, 2<sup>nd</sup> ed., Oxford University Press, New York, 2005, Chap. 5.
- <sup>9</sup>Filipski, M. N., Abdullah E. J., "Nanosatellite Navigation with the WMM2005 Geomagnetic Field Model," *Turkish Journal of Eng. Env. Sci.*, Vol. 30, 2006 pp. 43-55.
- <sup>10</sup>Wertz, J. R., Larson, W. J., *Space Mission Analysis and Design*, 3<sup>rd</sup> ed., Microcosm Press, Torrance CA, 1999 pp. 215.
- <sup>11</sup>Levesque, J., "Passive Magnetic Attitude Stabilization using Hysteresis Materials," Universite de Sherbrooke, SIGMA-PU-006-UdeS, Sept 2003. URL: <http://www.geocities.com/jflev/cubesim.htm> [cited 11 March 2007].
- <sup>12</sup>Morrish, A. H., *The Physical Principles of Magnetism*, IEEE Press, New York, 2001.
- <sup>13</sup>Menges, B. M., Guadamos, C. A., and Lewis, E. K., "Dynamic Modeling of Micro-Satellite Spartnik's Attitude," San Jose State University, Spartnik Satellite Project, Dec. 1996 SJSU. URL: <http://www.engr.sjsu.edu/spartnik/adac.html> [cited 12 March 2007].
- <sup>14</sup>Bate, R. R., Mueller, D. D., White, J. E., *Fundamentals of Astrodynamics*, Dover Publications, New York, 1971, Chap. 2.